## SUPPLEMENTAL INFORMATION

## SUPPLEMENTAL FIGURES

Figure S1

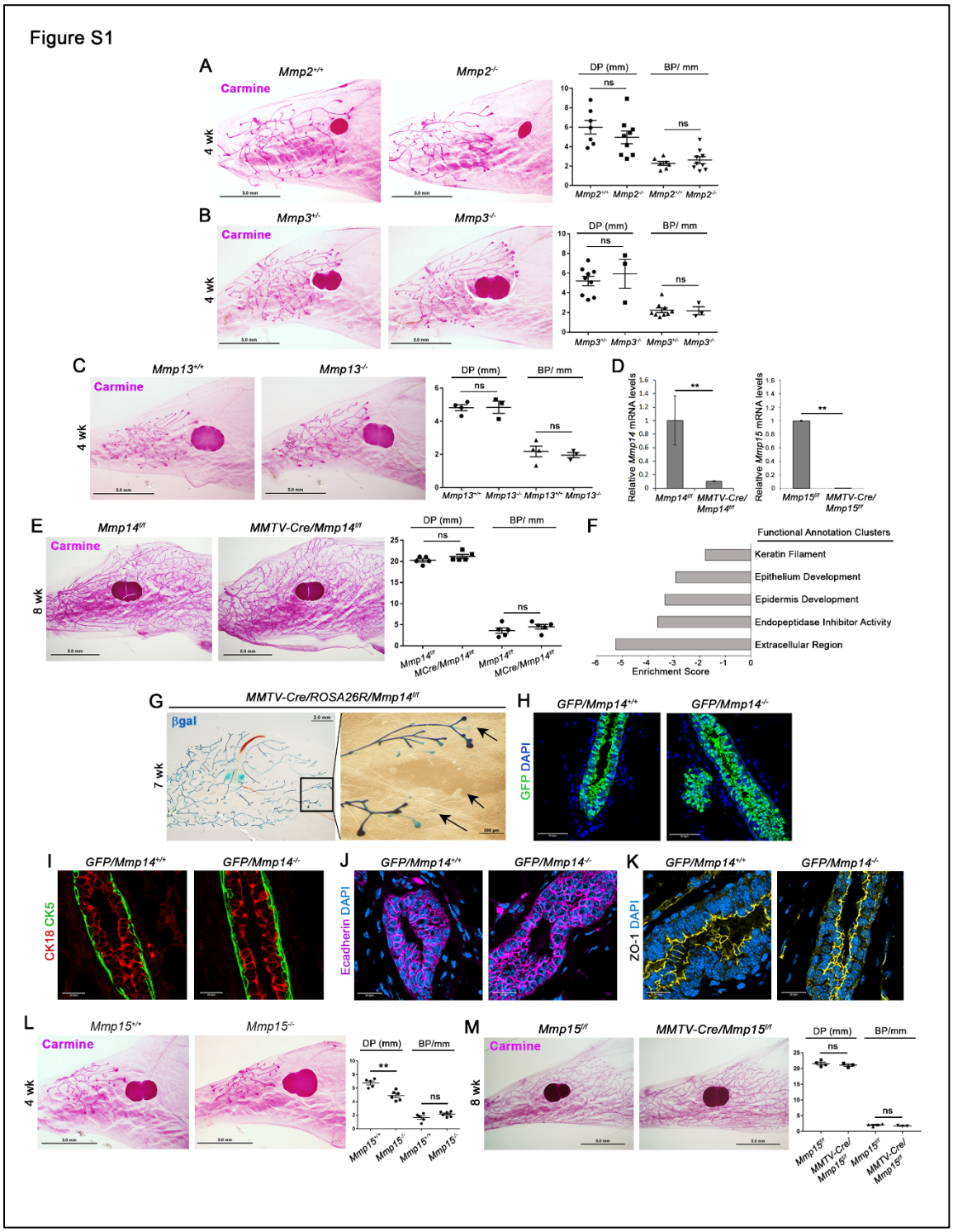

**Figure S1. Postnatal mammary gland branching proceeds independently of MMP2, MMP3 and MMP13 as well as epithelial cell-derived MT1-MMP and MT2-MMP *in vivo*, Related to Figure 1.**

(A) Carmine staining of mammary gland whole mounts from 4 week-old *Mmp2*$^{+/+}$ (n=7) and *Mmp2*$^{-/-}$ (n=9) mice with quantification of ductal penetration (DP) (mm) and branch points per mm duct (BP/mm). Data are presented as mean ± SEM.

(B) Carmine staining of whole mounts from 4 week-old *Mmp3*$^{+/-}$ (n=9) and *Mmp3*$^{-/-}$ (n=3) mice with quantification of DP (mm) and BP per mm duct. Data are presented as mean ± SEM.

(C) Carmine staining of whole mounts from 4 week-old *Mmp13*$^{+/+}$ (n=4) and *Mmp13*$^{-/-}$ (n=3) mice with quantifications of DP (mm) and BP per mm duct. Data are presented as mean ± SEM.

(A-C) Scale bar, 5.0 mm.

(D) QPCRs for *Mmp14* and *Mmp15* in mammary epithelial cells harvested from 4 week-old *Mmp14*$^{f/f}$ and *MMTV-Cre*$^{+/-}$*/Mmp14*$^{f/f}$ mice, and from 4 week-old *Mmp15*$^{f/f}$ and *MMTV-Cre*$^{+/-}$*/Mmp15*$^{f/f}$, as normalized to *Gapdh* (n=4, **p<0.001; mean ± SEM).

(E) Carmine-staining of mammary gland whole mounts isolated from 8 week-old *Mmp14*$^{fl/fl}$ and *MMTV-Cre*$^{+/-}$*/Mmp14*$^{f/f}$ mice (scale bar, 5.0 mm) with quantification of DP (mm) and BP per mm duct from n=5 mice per genotype. Data are presented as mean ± SEM.

(F) Chart of Functional Annotation Clusters and Gene ontology (GO) categories down-regulated in mammary epithelial cells harvested from 4 week-old *Mmp14*$^{f/f}$ and *MMTV-Cre*$^{+/-}$*/Mmp14*$^{f/f}$ mice (n=3 per genotype) with associated enrichment scores.

(G) LacZ staining of *MMTV-Cre*$^{+/-}$*/Mmp14*$^{fl/fl}$*/Rosa26R*$^{+/loxP}$ mammary gland whole mount from 7 week-old mice (scale bar, 2.0 mm). A box circumscribes the region at higher magnification (scale bar, 500 µm). Arrows indicate the wild-type (Cre-negative) ducts.

(H) GFP fluorescence with DAPI staining in mammary tissue cross-sections at 8 weeks post-transplantation of *Gfp*$^{+/-}$*/Mmp14*$^{+/-}$ and *Gfp*$^{+/-}$*/Mmp14*$^{-/-}$ ducts (scale bar, 50.0 µm).

(I-K) Immunofluorescence for CK18 and CK5 (I), E-cadherin (J) and Zonula occludens (ZO)-1 with DAPI staining (K) in mammary tissue cross-sections at 8 weeks post-transplantation of *Gfp*$^{+/-}$*Mmp14*$^{+/-}$ and *Gfp*$^{+/-}$*Mmp14*$^{-/-}$ ducts (scale bar, 20.0 µm).

(L) Carmine-staining of mammary gland whole mounts isolated from 4 week-old *Mmp15*$^{+/+}$ (n=5) and *Mmp15*$^{-/-}$ (n=6) mice (scale bar, 5.0 mm) with quantification of DP (mm) and BP per mm duct. Data are presented as mean ± SEM. (**p=0.0012)

(M) Carmine-staining of mammary gland whole mounts isolated from 8 week-old *Mmp15*$^{f/f}$ (n=4) *and MMTV-Cre*$^{+/-}$*/Mmp15*$^{f/f}$ mice (n=3) (scale bar, 5.0 mm) with quantification of DP (mm) and BP per mm duct. Data are presented as mean ± SEM.

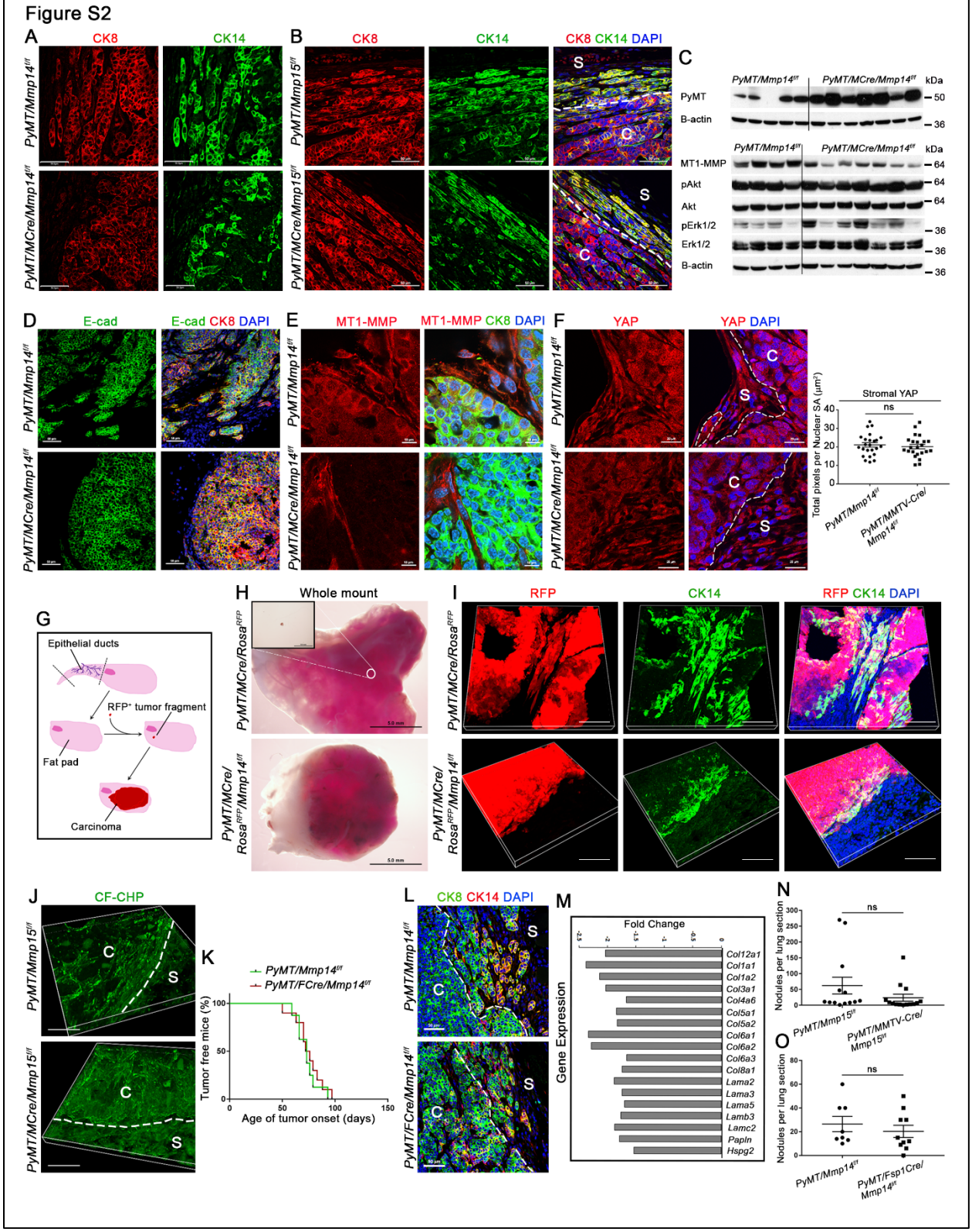
Figure S2
A
CK8
CK14
PyMT/Mmp14f/f
PyMT/MCre/Mmp14f/f
B
CK8
CK14
CK8 CK14 DAPI
PyMT/Mmp15f/f
PyMT/MCre/Mmp15f/f
S
C
C
PyMT/Mmp14f/f
PyMT/MCre/Mmp14f/f
kDa
PyMT
B-actin
50
36
MT1-MMP
pAkt
Akt
pErk1/2
Erk1/2
64
36
D
E-cad
E-cad CK8 DAPI
E
MT1-MMP
MT1-MMP CK8 DAPI
F
YAP
YAP DAPI
Stromal YAP
ns
Total pixels per Nuclear SA (µm²)
PyMT/Mmp14f/f
PyMT/MMTV-Cre/Mmp14f/f
G
Epithelial ducts
RFP+ tumor fragment
Fat pad
Carcinoma
H
Whole mount
PyMT/MCre/Rosa RFP
PyMT/MCre/Rosa RFP/Mmp14f/f
I
RFP
CK14
RFP CK14 DAPI
J
CF-CHP
K
PyMT/Mmp14f/f
PyMT/FCre/Mmp14f/f
Tumor free mice (%)
Age of tumor onset (days)
L
CK8 CK14 DAPI
PyMT/FCre/Mmp14f/f
M
Fold Change
Gene Expression
Col12a1
Col1a1
Col1a2
Col3a1
Col4a6
Col5a1
Col5a2
Col6a1
Col6a2
Col6a3
Col8a1
Lama2
Lama3
Lama5
Lamb3
Lamc2
Paplin
Hspg2
N
Nodules per lung section
PyMT/Mmp15f/f
PyMT/MMTV-Cre/Mmp15f/f
O
PyMT/Fsp1Cre/Mmp14f/f

**Figure S2. Carcinoma cell-derived MT1-MMP controls local invasion and metastasis independently of MT2-MMP or stromal cell-derived MT1-MMP, Related to Figure 2.**

(A) CK8 and CK14 immunofluorescence in mammary tumors harvested from 3-4 month-old *MMTV-PyMT$^{+/-}$/Mmp14$^{f/f}$* and *MMTV-PyMT$^{+/-}$/MMTV-Cre$^{+/-}$/Mmp14$^{f/f}$* mice (scale bar, 50.0 μm).

(B) CK8 and CK14 immunofluorescence with DAPI staining in mammary tumor cross-sections from 3-4 month-old *MMTV-PyMT$^{+/-}$/Mmp15$^{f/f}$* and *MMTV-PyMT$^{+/-}$/MMTV-Cre$^{+/-}$/Mmp15$^{f/f}$* mice (scale bar, 50.0 μm). Dotted lines mark the tumor-stromal interface. "S" indicates the stroma and "C" indicates the carcinoma in each section.

(C) Western blots for PyMT, MT1-MMP, pAkt, Akt, pErk1/2 and Erk1/2 in mammary tumors harvested from 3-4 month-old *MMTV-PyMT$^{+/-}$/Mmp14$^{f/f}$* and *MMTV-PyMT$^{+/-}$/MMTV-Cre$^{+/-}$/Mmp14$^{f/f}$* mice, as normalized to β-actin.

(D) Immunofluorescence of E-cadherin with CK8 and DAPI staining at the invasive edge of mammary tumor cross-sections from 3-4 month-old *MMTV-PyMT$^{+/-}$/Mmp14$^{f/f}$* and *MMTV-PyMT$^{+/-}$/MMTV-Cre$^{+/-}$/Mmp14$^{f/f}$* mice (scale bar, 50 μm).

(E) MT1-MMP immunofluorescence in 3-4 month-old *MMTV-PyMT$^{+/-}$/Mmp14$^{f/f}$* and *MMTV-PyMT$^{+/-}$/MMTV-Cre$^{+/-}$/Mmp14$^{f/f}$* mammary tumors (scale bar, 10 μm).

(F) Stromal cell YAP immunofluorescence in 3-4 month-old *MMTV-PyMT$^{+/-}$/Mmp14$^{f/f}$* and *MMTV-PyMT$^{+/-}$/MMTV-Cre$^{+/-}$/Mmp14$^{f/f}$* mammary tumors. Dotted line marks the tumor-stromal interface (scale bar, 20 μm). Quantification of the total pixels of YAP immunofluorescence per stromal cell nuclear surface area (μm$^2$) in n=4 tumors and n>20 fields per genotype. Data are presented as mean ± SEM.

(G) Cartoon of mammary tumor fragment transplantation.

(H) Whole mounts of RFP$^+$ tumors derived from *MMTV-PyMT$^{+/-}$/MMTV-Cre$^{+/-}$/Rosa$^{RFP}$* and *MMTV-PyMT$^{+/-}$/MMTV-Cre$^{+/-}$/Rosa$^{RFP}$/Mmp14$^{f/f}$* mammary tumor fragments at 7 weeks post-transplantation (scale bar, 5.0 mm). Inset shows tumor fragment before transplant

(scale bar, 5.0 mm). Circle drawn on tumor at 7 weeks indicates initial fragment size for comparison. Note the corrugated boundaries of the wild-type tumor mass relative to the conditional knockout.

(I) 3-D reconstructions of RFP fluorescence and CK14 immunofluorescence with DAPI staining in tumors derived from *MMTV-PyMT$^{+/-}$/MMTV-Cre$^{+/-}$/Rosa$^{RFP}$* and *MMTV-PyMT$^{+/-}$/MMTV-Cre$^{+/-}$/Rosa$^{RFP}$/Mmp14$^{f/f}$* mammary tumor fragments at 7 weeks post-transplantation (scale bar, 50 µm).

(J) 3-D reconstructions of CF-CHP immunofluorescence in mammary tumors harvested from 3-4 month-old *MMTV-PyMT$^{+/-}$/Mmp15$^{f/f}$* and *MMTV-PyMT$^{+/-}$/MMTV-Cre$^{+/-}$/Mmp15$^{f/f}$* mice. Dotted lines mark the tumor-stromal interface (scale bar, 30 µm).

(K) Kaplan-Meier plots depicting age of tumor onset (days) for *MMTV-PyMT$^{+/-}$/Mmp14$^{f/f}$* (n=12) versus *MMTV-PyMT$^{+/-}$/Fsp1-Cre$^{+/-}$/Mmp14$^{f/f}$* (n=13) mice.

(L) CK8 and CK14 immunofluorescence with DAPI staining in mammary tumor cross-sections from 3-4 month-old *MMTV-PyMT$^{+/-}$/Mmp14$^{f/f}$* and *MMTV-PyMT$^{+/-}$/Fsp1-Cre$^{+/-}$/Mmp14$^{f/f}$* mice (scale bar, 50 µm). Dotted lines mark the tumor-stromal interface.

(M) Changes in ECM transcriptomes in 3-4 month-old *MMTV-PyMT$^{+/-}$/Mmp14$^{f/f}$* and *MMTV-PyMT$^{+/-}$/MMTV-Cre$^{+/-}$/Mmp14$^{f/f}$* mammary tumors (n=4 per genotype).

(N) Quantification of lung nodules per cross-section in lungs harvested from *MMTV-PyMT$^{+/-}$/Mmp15$^{f/f}$* (n=13) and *MMTV-PyMT$^{+/-}$/MMTV-Cre$^{+/-}$/Mmp15$^{f/f}$* (n=14) mice. Data are presented as mean ± SEM.

**(O)** Quantification of lung nodules per cross-section in lungs harvested from *MMTV-PyMT$^{+/-}$/Mmp14$^{f/f}$* (n=8) and *MMTV-PyMT$^{+/-}$/Fsp1-Cre$^{+/-}$/Mmp14$^{f/f}$* (n=10) mice. Data are presented as mean ± SEM.

Figure S3

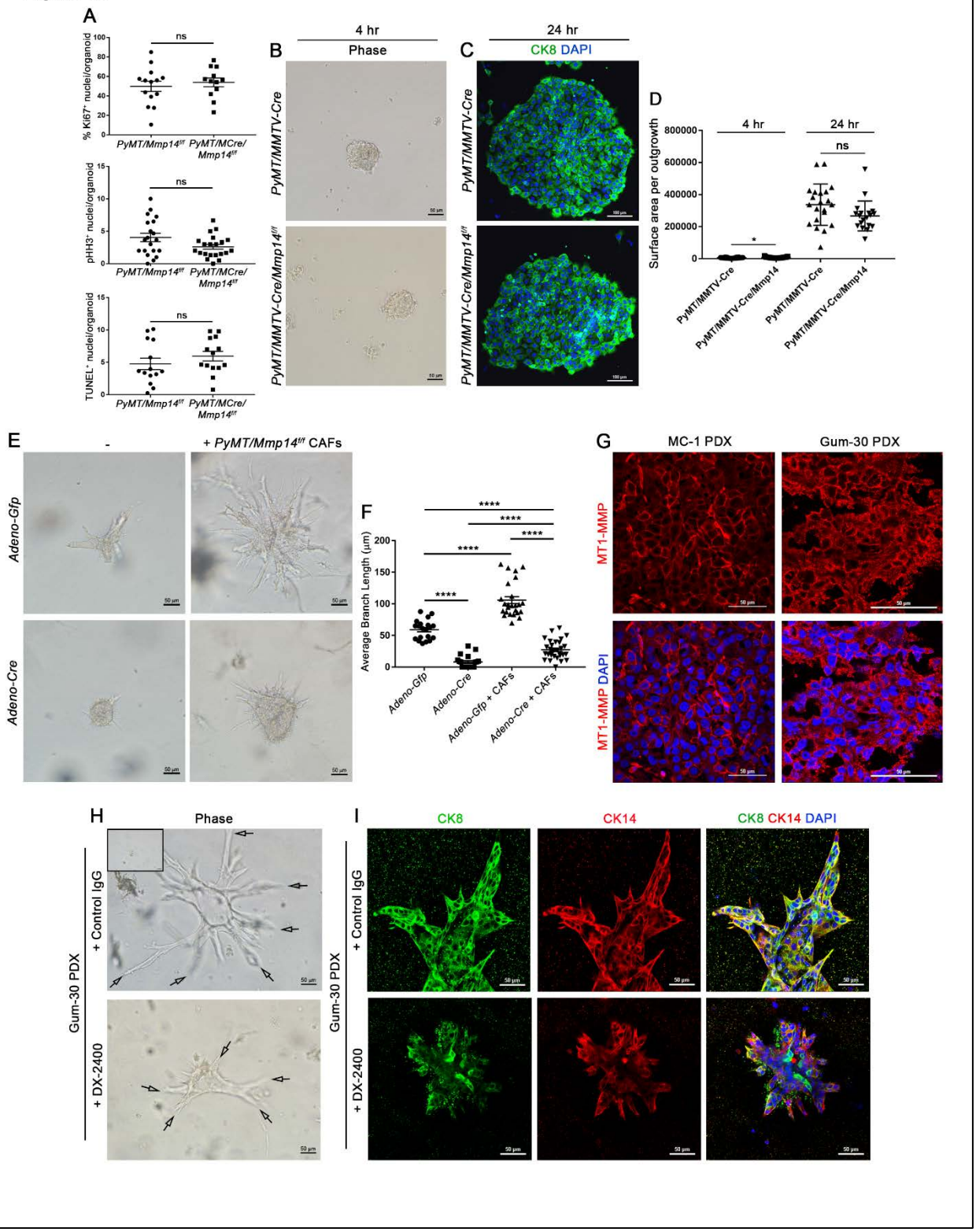
A
% Ki67+ nuclei/organoid
pHH3+ nuclei/organoid
TUNEL+ nuclei/organoid
ns
PyMT/Mmp14f/f
PyMT/MCre/Mmp14f/f
B
4 hr
Phase
PyMT/MMTV-Cre
PyMT/MMTV-Cre/Mmp14f/f
C
24 hr
CK8 DAPI
D
4 hr
24 hr
ns
*
Surface area per outgrowth
PyMT/MMTV-Cre
PyMT/MMTV-Cre/Mmp14
E
-
+ PyMT/Mmp14f/f CAFs
Adeno-Gfp
Adeno-Cre
F
Average Branch Length (μm)
****
Adeno-Gfp
Adeno-Cre
Adeno-Gfp + CAFs
Adeno-Cre + CAFs
G
MC-1 PDX
Gum-30 PDX
MT1-MMP
MT1-MMP DAPI
H
Phase
Gum-30 PDX
+ Control IgG
+ DX-2400
I
CK8
CK14
CK8 CK14 DAPI
Gum-30 PDX
+ Control IgG
+ DX-2400

**Figure S3. MT1-MMP directs both mouse and human breast carcinoma invasion programs *ex vivo*, Related to Figure 3.**

(A) Quantification of the percentage of Ki67-positive nuclei per organoid (n≥12 per genotype) (top panel), the number of phospho-histone H3 (pHH3)-positive nuclei per organoid (n≥20 per genotype) (middle panel), and the number of TUNEL-positive nuclei per organoid (n=14 per genotype) (lower panel) in *MMTV-PyMT$^{+/-}$/Mmp14$^{f/f}$* and *MMTV-PyMT$^{+/-}$/MMTV-Cre$^{+/-}$/Mmp14$^{f/f}$* mammary carcinoma-derived organoids after 3 days of culture within 3-D type I collagen with FGF-2. Data are presented as mean ± SEM.

(B) Bright-field micrographs of *MMTV-PyMT$^{+/-}$/Mmp14$^{f/f}$* and *MMTV-PyMT$^{+/-}$/MMTV-Cre$^{+/-}$/Mmp14$^{f/f}$* mammary carcinoma-derived organoids cultured atop a 3-D type I collagen hydrogel with FGF-2 at 4 hours.

(C) CK8 immunofluorescence with DAPI counter-staining in *MMTV-PyMT$^{+/-}$/Mmp14$^{f/f}$* and *MMTV-PyMT$^{+/-}$/MMTV-Cre$^{+/-}$/Mmp14$^{f/f}$* mammary carcinoma-derived organoids after 24 hours of culture atop a 3-D type I collagen hydrogel with FGF-2.

(D) Quantification of *MMTV-PyMT$^{+/-}$/Mmp14$^{f/f}$* and *MMTV-PyMT$^{+/-}$/MMTV-Cre$^{+/-}$/Mmp14$^{f/f}$* mammary carcinoma-derived organoid surface area at 4 hours and following outgrowth at 24 hours (n≥30 at 4 hours and n≥20 at 24 hours from representative experiment). (*p=0.0141 with *MMTV-PyMT$^{+/-}$/Mmp14$^{f/f}$* at 5813 ± 433.5 μm$^2$ and *MMTV-PyMT$^{+/-}$/MMTV-Cre$^{+/-}$/Mmp14$^{f/f}$* at 7622 ± 570.9 μm$^2$).

(E) Bright-field micrographs of mammary carcinoma-derived organoids harvested from 3 month-old *MMTV-PyMT$^{+/-}$/Mmp14$^{f/f}$* mice and transduced with either Adenoviral-GFP or Adenoviral-Cre prior to embedding in 3-D type I collagen for 3 days with FGF-2 in the presence or absence of *MMTV-PyMT$^{+/-}$/Mmp14$^{f/f}$* tumor-derived CAFs (scale bar, 50 μm).

(F) Quantifications of tumor organoid invasion, as represented by the average branch length (μm) of the three longest branches (****p<0.0001; n≥19 for organoid alone conditions and n ≥ 25 for co-culture conditions). Data are presented as mean ± SEM.

(G) MT1-MMP immunofluorescence with DAPI staining in cross-sections from intact human patient-derived xenograft (PDX) tumors MC-1 and Gum30 (scale bar, 50 μm).

(H) Bright-field micrographs of organoids harvested from PDX Gum30 tumors and embedded within 3-D type I collagen for 4 days with FGF-2 in the presence of the anti-MT1-MMP antibody (DX-2400) or a control IgG antibody (scale bar, 50 μm). Inset shows bright-field micrograph of Gum30 organoid at time 0. Arrows mark terminal ends of branching structures. Organoid branch length is reduced from 150.5±7.7 μm with 8.8±0.9 branches/organoid in the presence of control IgG (n=18) to 65.0±6.1 μm with 4.9±0.6 branches/organoid in the presence of DX-2400 (n=15) ($p \leq 0.001$, mean ± SEM).

(I) CK8 and CK14 immunofluorescence with DAPI staining in organoids harvested from PDX Gum30 tumors and embedded within 3-D type I collagen for 4 days with FGF-2 in the presence of DX-2400 antibody or control IgG antibody (scale bar, 50 μm).

Figure S4

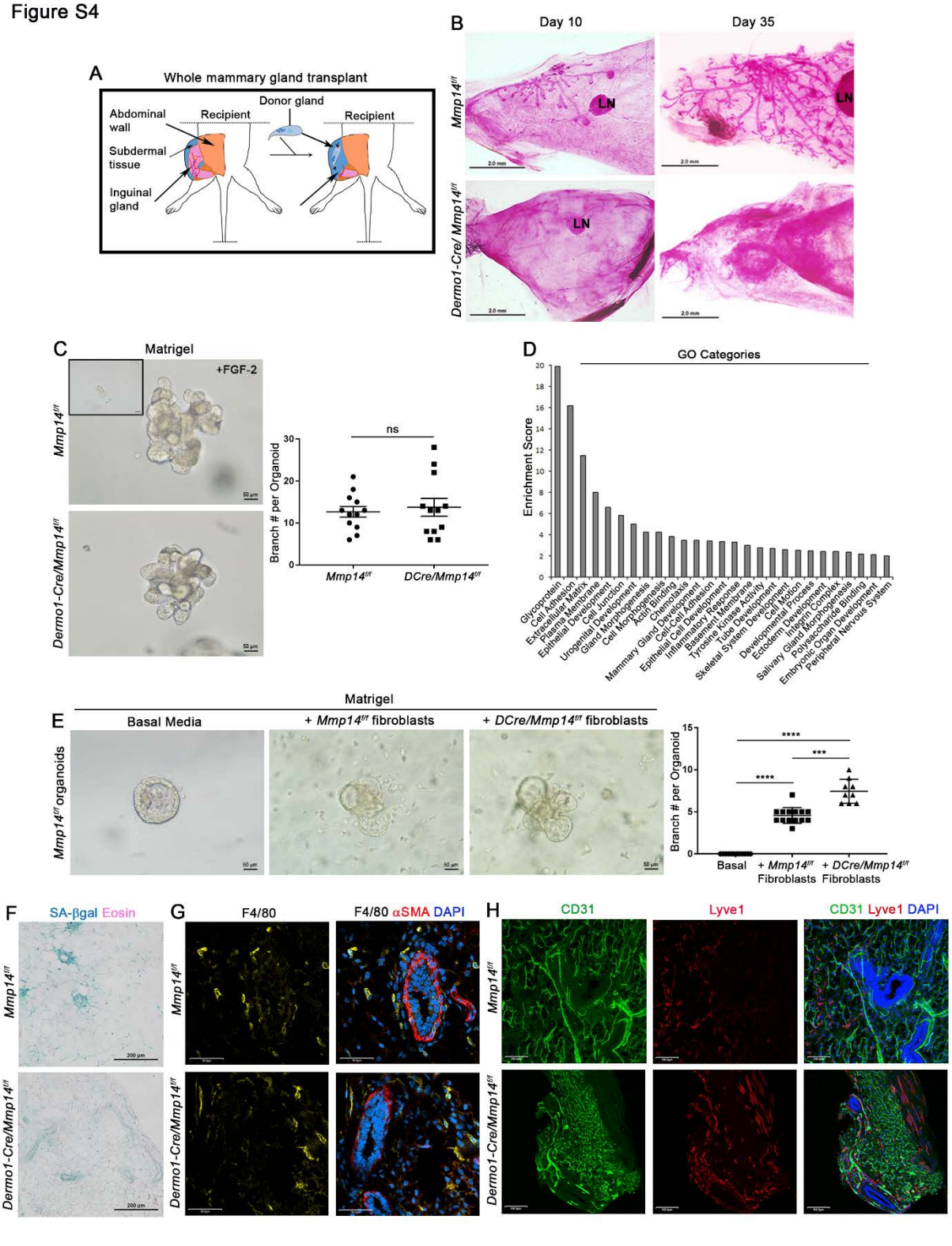
A
Whole mammary gland transplant
Donor gland
Abdominal wall
Recipient
Recipient
Subdermal tissue
Inguinal gland
B
Day 10
Day 35
Mmp14f/f
Dermo1-Cre/ Mmp14f/f
LN
C
Matrigel
+FGF-2
Mmp14f/f
Dermo1-Cre/Mmp14f/f
Branch # per Organoid
ns
Mmp14f/f
DCre/Mmp14f/f
D
GO Categories
Enrichment Score
Glycoprotein
Cell Adhesion
Extracellular Matrix
Plasma Membrane
Epithelial Development
Cell Junction
Urogenital Development
Gland Morphogenesis
Cell Morphogenesis
Actin Binding
Chemotaxis
Mammary Gland Development
Cell-Cell Adhesion
Epithelial Cell Development
Inflammation Response
Basement Membrane
Tyrosine Kinase Activity
Tube Development
Skeletal System Development
Cell Motion
Developmental Process
Integrin Complex
Ectoderm Development
Polysaccharide Binding
Salivary Gland Morphogenesis
Embryonic Organ Development
Peripheral Nervous System
E
Matrigel
Basal Media
+ Mmp14f/f fibroblasts
+ DCre/Mmp14f/f fibroblasts
Mmp14f/f organoids
Branch # per Organoid
Basal
+ Mmp14f/f Fibroblasts
+ DCre/Mmp14f/f Fibroblasts
F
SA-βgal Eosin
Mmp14f/f
Dermo1-Cre/Mmp14f/f
G
F4/80
F4/80 αSMA DAPI
Mmp14f/f
Dermo1-Cre/Mmp14f/f
H
CD31
Lyve1
CD31 Lyve1 DAPI
Mmp14f/f
Dermo1-Cre/Mmp14f/f

**Figure S4. Stromal cell-derived MT1-MMP controls mammary gland branching in an organ autonomous fashion independent of stromal cell-derived growth factors, macrophages or endothelial cells, Related to Figure 5.**

(A) Schematic of whole mammary gland transplant procedure.

(B) Carmine-stained whole mounts of transplanted donor mammary glands from *Mmp14*$^{f/f}$ or *Dermo1-Cre*$^{+/-}$*/Mmp14*$^{f/f}$ mice at 10 days and 5 weeks post-transplantation (scale bar, 2.0 mm). “LN” indicates donor inguinal lymph node.

(C) Bright-field micrographs of mammary epithelial organoids harvested from 6 week-old *Mmp14*$^{f/f}$ and *Dermo1-Cre*$^{+/-}$*/Mmp14*$^{f/f}$ mice and cultured within Matrigel with FGF-2 with quantification of branch number per organoid from n=12 fields per genotype (scale bar, 50 μm). Data are presented as mean ± SEM. Inset shows bright-field micrograph of organoid at time 0.

(D) Gene ontology (GO) categories differentially expressed in 4 week-old *Dermo1-Cre*$^{+/-}$*/Mmp14*$^{f/f}$ and wild-type mammary tissue (n=3 per genotype).

(E) Bright-field micrographs of mammary epithelial organoids harvested from 6 week-old *Mmp14*$^{f/f}$ mice and cultured within Matrigel alone under basal conditions (without FGF-2) (left panel), in the presence of 100 *Mmp14*$^{f/f}$ fibroblasts per organoid (middle panel), or in the presence of 100 *Dermo1-Cre*$^{+/-}$*/Mmp14*$^{f/f}$ fibroblasts per organoid (right panel) (scale bar, 50 μm) with quantification of branch number per organoid (***p=0.0002, ****p<0.0001).

(F) Senescence-associated β-galactosidase (SA-βgal) staining (pH 6.0) of mammary gland cross-sections from 4 week-old *Mmp14*$^{f/f}$ and *Dermo1-Cre*$^{+/-}$*/Mmp14*$^{f/f}$ mice with Eosin counter-staining (scale bar, 200 μm).

(G) F4/80 with α-smooth muscle actin (αSMA) immunofluorescence to delineate the myoepithelial cell compartment and DAPI staining (scale bar, 50 μm) in *Mmp14*$^{f/f}$ and *Dermo1-Cre*$^{+/-}$*/Mmp14*$^{f/f}$ mammary gland cross-sections.

(H) CD31 (vascular endothelial cells) and Lyve1 (lymphatic endothelial cells) immunofluorescence with DAPI staining in *Mmp14*$^{f/f}$ and *Dermo1-Cre*$^{+/-}$*/Mmp14*$^{f/f}$ mammary gland cross-sections (scale bar, 100μm).

Figure S5

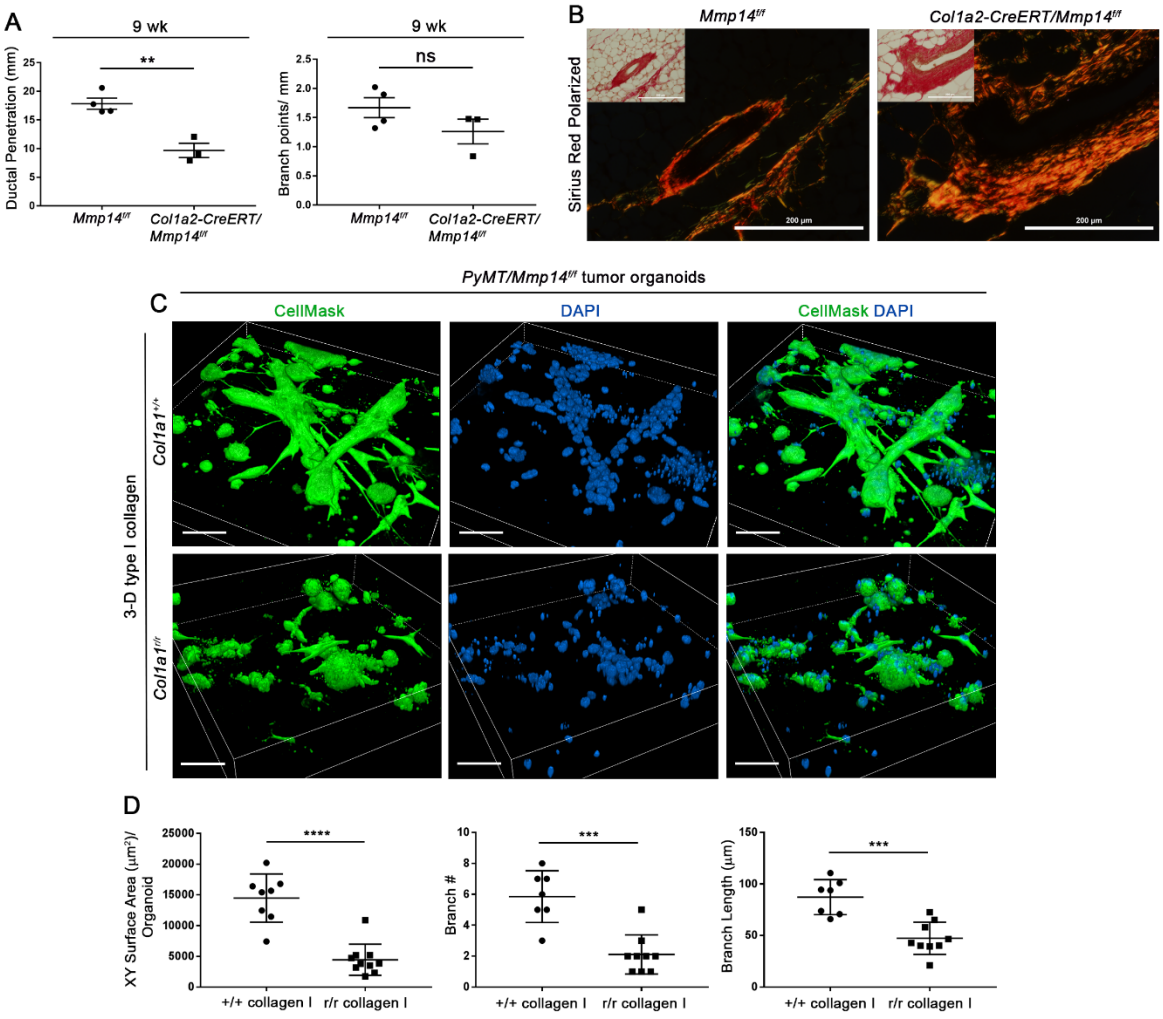
A
9 wk
**
Ductal Penetration (mm)
Mmp14f/f
Col1a2-CreERT/ Mmp14f/f
9 wk
ns
Branch points/ mm
Mmp14f/f
Col1a2-CreERT/ Mmp14f/f
B
Mmp14f/f
Col1a2-CreERT/Mmp14f/f
Sirius Red Polarized
200 µm
200 µm
PyMT/Mmp14f/f tumor organoids
C
CellMask
DAPI
CellMask DAPI
3-D type I collagen
Col1a1+/+
Col1a1f/f
D
XY Surface Area (µm²)/ Organoid
****
+/+ collagen I
r/r collagen I
Branch #
***
+/+ collagen I
r/r collagen I
Branch Length (µm)
***
+/+ collagen I
r/r collagen I

**Figure S5. Postnatal mammary gland branching requires type I collagen remodeling by periductal fibroblasts while invading carcinoma cells directly remodel type I collagen, Related to Figure 6.**

(A) Quantification of ductal penetration (mm) and branch points per mm duct in 9 week-old mammary glands harvested from *Mmp14$^{f/f}$* (n=4) and *Col1a2-CreERT$^{+/-}$/Mmp14$^{f/f}$* (n=3) (**p=0.006).

(B) Polarized light images of Sirius Red staining of 9 week-old *Mmp14$^{f/f}$* and *Col1a2-CreERT$^{+/-}$/Mmp14$^{f/f}$* glands (scale bar, 200 µm). Insets show corresponding bright-field images.

(C) 3-D reconstructions of *MMTV-PyMT$^{+/-}$/Mmp14$^{f/f}$* mammary tumor organoids within 3-D type I collagen extracted from *Col1a1$^{+/+}$* or *Col1a1$^{r/r}$* mouse tails and labeled with CellMask dye and DAPI after 4 days of culture with FGF-2. Carcinoma cells invade 3-D hydrogels of native, but not mutant, type I collagen (scale bar, 50 µm).

(D) Quantifications of XY surface area (um$^2$), branch number and branch length (um) of organoids cultured within *Col1a1$^{+/+}$* or *Col1a1$^{r/r}$* type I collagen for 4 days with FGF-2 (****p<0.0001, ***p≤0.0005).

## SUPPLEMENTAL TABLES

**Table S1. Differential expression of epithelium-associated genes in array of *Mmp14*-targeted mammary epithelial cells, Related to Figure 1.**

| Gene | Fold change |
|---|---|
| *Glycam1* | -40.9 |
| *Csn1s1* | -6.99 |
| *Csn2* | -5.31 |
| *Sprr2a3* | -4.77 |
| *Sprr2a1* | -2.99 |
| *Csn1s2a* | -2.39 |
| *Epgn* | -2.07 |
| *Wfdc21* | -2.06 |
| *Krt1* | -2.03 |
| *Krt10* | -1.95 |
| *Sprr2e* | -1.80 |
| *Sprr1b* | -1.78 |
| *Lalba* | -1.77 |
| *Muc13* | -1.56 |
| *Krt6b* | -1.53 |
| *Areg* | -1.52 |
| *Sprr1a* | -1.52 |

**Table S1.** Differential expression of epithelium-associated genes in Affymetrix microarray of mammary epithelial organoids isolated from *MMTV-Cre*$^{+/-}$*/Mmp14*$^{f/f}$ female mice (n=2), as compared to *Mmp14*$^{f/f}$ female littermates (n=3).

**Table S2. Genotyping PCR Primers, Related to the STAR Methods Section.**

| Allele | Forward (5' to 3') | Reverse (5' to 3') |
|---|---|---|
| *Mmp14*$^{KO}$ | *Mmp14*$^{WT}$: CTAGGCCTGGAACAT TCTAACGATC<br>*Mmp14*$^{KO}$*:* GTGCGAGGCCAGAGGC CACTTGTGT | *Mmp14*$^{R}$: CTTTGTGGGTGACCCTGACTTGC |
| *Mmp14*$^{lacZ}$ | *Mmp14*$^{lacZ}$*(+)*: ACCTGCGTGCAATCCATCTTG<br>*Mmp14*$^{lacZ}$*(-)*: TGAGGTGGAAAACACGACCAG | *Mmp14*$^{lacZ}$: ATGATGGCGGAGGGATCGTTAG |

| | | |
|---|---|---|
| *Mmp15*$^{KO}$ | *Mmp15*$^{WT}$: CCGCCACCAAGCCTC ACTGTCT<br>*Mmp15*$^{KO}$: CGCCACCAAGCCTCA CTGTCT | *Mmp15*$^{WT}$: AAAGCCACCCACGCC ATCAAAC<br>*Mmp15*$^{KO}$: AATTGCTGGGGATGG AGGAAGGTA |
| *Mmp15*$^{lacZ}$ | GAGATGGCGCAACGCAATTAATG | TGCACGTCCCATTCTCATGC |
| *Mmp2*$^{KO}$ | *Mmp2*$^{WT}$: GTGCTACTGCAGGATA AACTGATG<br>*Mmp2*$^{KO}$: GCGCCTACCGGTGGA TGTGGAATGTGTGCG | *Mmp2*$^{WT}$: CCGGGACAGGAACGTA CTGGGTTC<br>*Mmp2*$^{KO}$: CCGGGACAGGAACGTA CTGGGTTC |
| *Mmp3*$^{KO}$ | *Mmp3*$^{WT}$: ACCGGATTTGCCAAG ACAGAGTG | *Mmp3*$^{WT}$: GCATCTCCATTAATCCC TGGTCC |
| *Mmp13*$^{KO}$ | *Mmp13*$^{WT}$*:* TTGGCCACTCCCTAGGTCT | *Mmp13*$^{WT}$*:* CTACCCAGACAAGCAGTTTGC |
| *Neo* | AGGATCTCCTGTCATCTCAC CTTGCTCCTG | AAGAACTCGTCAAGAAGG CGATAGAAGGCG |
| *Mmp14*$^{flox}$ | GTTGAGGCAGGAGGATTGTGAGTT | CCTGGAAAAGTGGGCGAGAAG |
| *iCre* | CCGTTTGCCGGTCGTGGG | CGAATATCCTGGCAGCGATC |
| *MMTV-Cre* | GGTTCT GATCTGAGCTCTGAGTG | CATCACTCGTTGCATCGACCGG |
| *PyMT* | Internal Control (oIMR8744): CAAATGTTGCTTGTCTGGTG Trangene (oIMR0384): GGAAGCAAGTACTTCACAAGGG | Internal Control (oIMR8745): GTCAGTCGAGTGCACAGTTT Transgene (oIMR0385): GGAAAGTCACTAGGAGCAGGG |
| *Fsp1-Cre* | ATGCTTCTGTCCGTTTGCCG | CAATGCGATGCAATTTCCTC |
| *Col1a1*$^{r}$ | TGGTTCTGGAATGAGGATGG | TGCCTCTGCTTCCTTAGTGC |

**Table S3. Quantitative real-time PCR primers, Related to the STAR Methods Section.**

| Gene | Forward (5’ to 3’) | Reverse (5’ to 3’) |
|---|---|---|
| *Gapdh* | TGAAGCAGGCATCTGAGGG | CGAAGGTGGAAGAGTGGGAG |
| *Arbp* | CACTGGTCTAGGACCCGAGAA | AGGGGGAGATGTTCAGCATGT |
| *Mmp14* | CTGCCATTGCCGCCATGCAAAA | TGGCGTGGCACTCTCCCATACT |
| *Mmp15* | ACATGTCCACCATGCGCTCT | TACCATGATGTCAGCCTCC |
| *Mmp2* | TCTGGAGCGAGGATACCCCAA | TTCCAGGAGTCTGCGATGAGC |
| *Mmp3* | GTTCCTGATGTTGGTGGCTT | AGCCTCTCCTTCAGAGATCC |
| *Mmp13* | CTTTTCCTCCTGGACCAAACT | TCATGGGCAGCAACAATAAA |